

# OPTIMIZED LEARNED ENTROPY CODING PARAMETERS FOR PRACTICAL NEURAL-BASED IMAGE AND VIDEO COMPRESSION

Amir Said    Reza Pourreza    Hoang Le

Qualcomm AI Research,\* San Diego, CA, USA

## ABSTRACT

Neural-based image and video codecs are significantly more power-efficient when weights and activations are quantized to low-precision integers. While there are general-purpose techniques for reducing quantization effects, large losses can occur when specific entropy coding properties are not considered. This work analyzes how entropy coding is affected by parameter quantizations, and provides a method to minimize losses. It is shown that, by using a certain type of coding parameters to be learned, uniform quantization becomes practically optimal, also simplifying the minimization of code memory requirements. The mathematical properties of the new representation are presented, and its effectiveness is demonstrated by coding experiments, showing that good results can be obtained with precision as low as 4 bits per network output, and practically no loss with 8 bits.

**Index Terms**— Learned image and video compression, neural network quantization, entropy coding.

## 1. INTRODUCTION

After years of research showing the advantages of neural-based techniques for video coding [1, 2], and recent demonstrations of real-time decoding in mobile devices [3, 4], there is growing interest in their standardization and commercial deployment [5], and a main practical implementation challenge is the minimization of decoding power requirements.

Implementing neural network (NN) computations with low-precision integers significantly reduces power needs, but requires minimizing the effects of quantizing networks weights and activations [6, 7, 8]. For neural image and video codecs, efficacy is strongly defined by the entropy coding stage and related networks, and can be severely degraded.

Analyzing quantization effects in NNs can be difficult because they implement non-linear processes, and learned variables have unknown properties. Techniques based on re-training under quantization constraints help to reduce the losses, but have limited efficacy.

In this work it is shown that NN outputs used for entropy coding have well-defined meaning and properties, which can be used for predicting quantization effects. Furthermore, those properties can be used for modifying the loss function

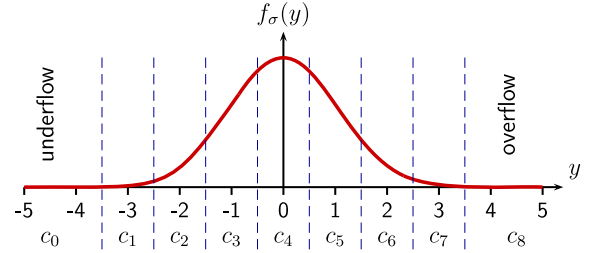


**Fig. 1.** Quantized values from normal distribution with std. dev.  $\sigma$ , commonly used in neural-based codecs.

used while learning, and it is demonstrated that networks can be trained to be minimally sensitive to quantization.

Further analysis shows that this optimized representation is remarkably independent of the quantization, and thus networks do not need to be retrained even after significant changes to entropy coding design choices. Thus, in those networks the uniform quantization can also be extended beyond the hardware requirements, and used to minimize the memory needed for storing entropy coding tables.

Experimental results show that the proposed solution can guarantee good performance ( $\approx 2\%$  redundancy) with precision as low as 4 bits, and with relative redundancy reduction by a factor of 4 for each additional bit, reaching less than 0.01% for 8 bits.

## 2. ENTROPY CODING FOR NN-BASED CODECS

Entropy coding in conventional codecs is based on estimating the probabilities of variables to be coded. For example, in video standards like HEVC and VVC [9, 10, 11], adaptive binary arithmetic coding contexts are used for estimating probabilities related to data elements.

Neural-based codecs use a different principle: a parameterized probability distribution (pdf) is chosen for training, and a learned scheme (table or NN) is used to determine the parameter value to be used for coding a quantized random variable. Fig. 1 shows an example of the commonly used normal distribution, and unit-step quantization.

The sequence of probabilities of random variable  $y \sim \mathcal{N}(0, \sigma^2)$ , quantized to value  $n \in \mathbb{Z}$ , is

$$p_n(\sigma) = \frac{1}{2} \left[ \operatorname{erfc} \left( \frac{2n-1}{\sqrt{8}\sigma} \right) - \operatorname{erfc} \left( \frac{2n+1}{\sqrt{8}\sigma} \right) \right], \quad (1)$$

\*Qualcomm AI Research is an initiative of Qualcomm Technologies, Inc.

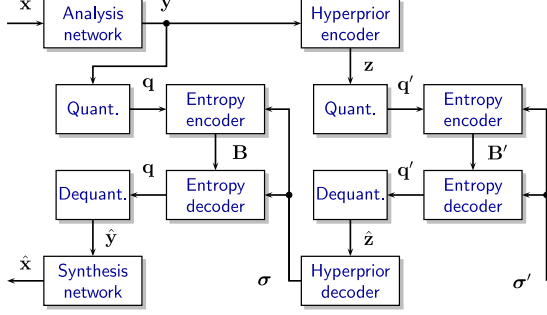


**Fig. 2.** Example of a neural-based codec architecture, including scale hyperprior networks for entropy coding.

with entropy

$$H(\sigma) \stackrel{\text{def}}{=} - \sum_{n=-\infty}^{\infty} p_n(\sigma) \log_2(p_n(\sigma)), \quad (2)$$

where the *complementary error function* is

$$\text{erfc}(x) \stackrel{\text{def}}{=} \frac{2}{\sqrt{\pi}} \int_x^{\infty} e^{-t^2} dt. \quad (3)$$

In practical implementations special symbols are used to code values in *underflow* and *overflow* infinite sets, which have very small but nonzero probabilities, as shown in Fig. 1. Within those sets the values are sub-optimally coded with, for example, Elias universal codes [12].

Also shown in Fig. 1 are the elements of *code vector*  $\mathbf{c}(\sigma)$  (CV), which contain the probabilities to be used for arithmetic coding (AC), within a given range  $R$

$$c_i(\sigma) = \begin{cases} \sum_{n=-\infty}^{-R} p_n(\sigma), & i = 0, \\ p_{i-R}(\sigma), & i = 1, 2, \dots, 2R - 1, \\ \sum_{n=R}^{\infty} p_n(\sigma), & i = 2R. \end{cases} \quad (4)$$

To simplify the notation we ignore implementation details like conversions to integer-valued cumulative sums for AC [13, 14]. It is assumed that  $R$  and AC precision are chosen to obtain compression very close to entropy.

This type of entropy coding is used within a NN-based codec as shown in Fig. 2, corresponding to the scale hyperprior architecture [15]. There are other codec configurations, but our main interest is in the per-element coding stages shown in Fig. 3, which is used with all factorized priors.

The latent  $y$  to be coded is quantized with  $Q_{y \rightarrow q}$ , which is taken into account during floating-point training. The problems addressed here are caused by the quantization stage  $Q_{\sigma \rightarrow \hat{\sigma}}$ , representing the use of low-precision network outputs during coding, but not during training.

Since code vectors must be bitwise identical at the encoder and decoder [16], given a range  $\mathcal{U} = [\sigma_{\min}, \sigma_{\max}]$ , we assume they share a monotonic sequence  $\{t_k\}_{k=0}^N$  partitioning  $\mathcal{U}$ , and that latent  $y$  is coded using  $\mathbf{c}(\rho_k^*)$  whenever  $\hat{\sigma} \in [t_k, t_{k+1})$ .

To determine the optimal values of  $\rho_k^*$  for code vector computation we measure the *average redundancy*, defined by

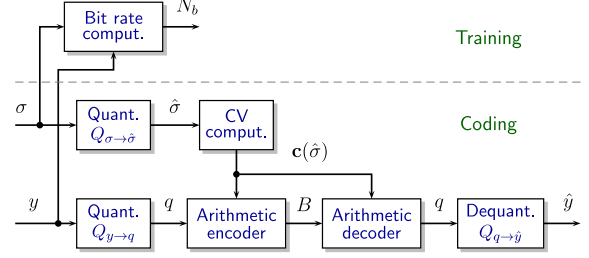


**Fig. 3.** Per-element entropy coding, including quantization of pdf parameter  $\sigma$ .

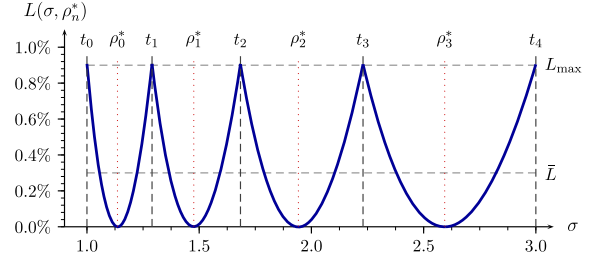


**Fig. 4.** Example of nonuniform quantization of parameter  $\sigma$ , designed for constant maximum relative redundancy.

the Kullback-Leibler divergence

$$R(\sigma, \rho) \stackrel{\text{def}}{=} \sum_{n=-\infty}^{\infty} p_n(\sigma) \log_2 \left( \frac{p_n(\sigma)}{p_n(\rho)} \right). \quad (5)$$

Since practical image and video codecs are meant to be efficient in a wide range of bit rates, it is interesting to have entropy coding designed to minimize *relative redundancy*

$$L(\sigma, \rho) \stackrel{\text{def}}{=} \frac{R(\sigma, \rho)}{H(\sigma)}. \quad (6)$$

and to enable good performance for all use cases use

$$\rho_k^* = \arg \min_{\rho} \int_{t_k}^{t_{k+1}} L(\sigma, \rho) d\sigma. \quad (7)$$

### 3. NEW PDF PARAMETERIZATION

From these definitions it is possible to optimize non-uniform quantization schemes as shown in the example of Fig. 4, where similarly to other quantization solutions, all intervals have the same maximum relative redundancy and averages

$$\bar{L}_k \stackrel{\text{def}}{=} \frac{1}{t_{k+1} - t_k} \int_{t_k}^{t_{k+1}} L(\sigma, \rho_k^*) d\sigma. \quad (8)$$

With sufficiently fine quantization of  $\sigma$ ,  $L(\sigma, \rho_k^*)$  is approximately quadratic, and we can use

$$\rho_k^* \approx \{\rho : L(t_k, \rho) = L(t_{k+1}, \rho)\}, \quad (9)$$

$$\bar{L}_k \approx \frac{L(t_k, \rho_k^*)}{3} = \frac{L(t_{k+1}, \rho_k^*)}{3}. \quad (10)$$

Neural-based codecs using precise floating-point computations can be implemented with arrays of pre-computed

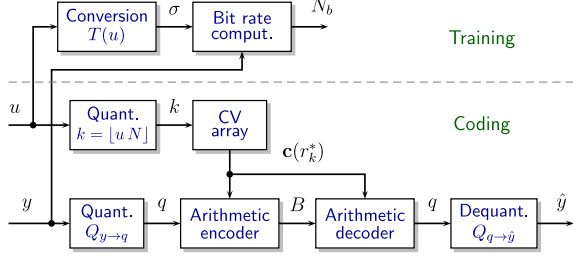


**Fig. 5.** Proposed modification of codec in Fig. 3, replacing pdf parameter  $\sigma$  with parameter  $u$  optimized for quantization.

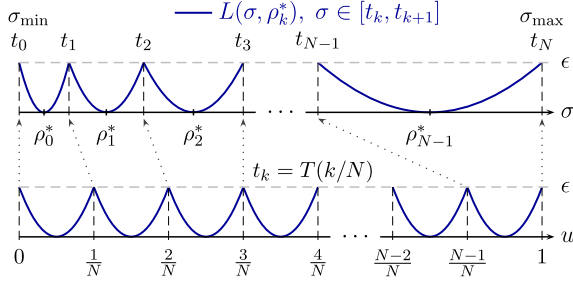


**Fig. 6.** Mapping from non-uniform to uniform quantization.

code vectors, and the approach shown in the example of Fig. 4. However, for practical codecs, which must handle a wide range of bit rates, it is necessary to support, for example,  $\sigma \in [0.1, 1000]$  with the precision of hyperprior network output  $\hat{\sigma}$  constrained to only 8 bits. This means that  $\{t_k\}_{k=0}^N$  must also use only 8 bits, severely constraining the design and resulting in significant losses.

To solve this problem we can exploit the fact that  $\sigma$  is only used for rate estimation during training, and while computing code vectors. The proposed solution is shown in Fig. 5: hyperprior networks are trained to compute a new pdf parameter  $u \in [0, 1]$  that is converted as  $\sigma = T(u)$ . For analysis we define  $u \in \mathbb{R}$ , but note that during actual coding the quantized networks only need to generate integer  $k$ . This approach is used in [16], where the conversion is chosen to be in the form  $\sigma = e^{\alpha u + \beta}$ .

Fig. 6 shows how optimal  $T(u, N)$  can be defined, for a given  $N$ , to obtain constant maximum relative redundancy, and the following algorithm can be used for its computation.

1. Given  $N$  and  $[\sigma_{\min}, \sigma_{\max}]$ , choose initial maximum redundancy  $\epsilon$ ; initialize  $t_0 = \sigma_{\min}$ .
2. For  $n = 1, 2, \dots, N$ :
  - (a) Set  $\rho_{n-1}^* = \{\rho > t_{n-1} : L(t_{n-1}, \rho) = \epsilon\}$ ;
  - (b) Set  $t_n = \{t > \rho_{n-1}^* : L(t, \rho_{n-1}^*) = \epsilon\}$ .
3. If  $t_N \approx \sigma_{\max}$  then stop.
4. If  $t_N < \sigma_{\max}$  then increase  $\epsilon$ , otherwise decrease  $\epsilon$ , using a method for unidimensional search.
5. Go to step 2.

The surprising conclusion from computing  $T(u, N)$  for several values of  $N$ , and interpolating between the sampled values, is that all results are practically identical. This means that if we compute

$$T(u) = \lim_{N \rightarrow \infty} T(u, N), \quad (11)$$

we obtain a single reference function that can be used for all network trainings, and the value of  $N$  can be chosen and modified later, without the need for re-training.

The rationale for determining  $T(u)$  can be seen from the lower part of Fig. 6. For increasing values of  $N$  the redundancy curves in all intervals should approximate quadratic equations on  $u$ , with same second derivatives. This can be achieved if we can find  $T(u)$  and constant  $\alpha$  such that

$$\left. \frac{\partial^2}{\partial u^2} L(T(u), \rho) \right|_{\rho=T(u)} = \alpha, \quad u \in [0, 1]. \quad (12)$$

Defining

$$\psi(\sigma) \stackrel{\text{def}}{=} \left. \frac{\partial^2}{\partial \sigma^2} L(\sigma, \rho) \right|_{\rho=\sigma} \quad (13)$$

it can be shown that, thanks to properties of  $L(\sigma, \rho)$ , eq. (12) is equivalent to

$$\frac{d}{du} T(u) = \sqrt{\frac{\alpha}{\psi(T(u))}}, \quad (14)$$

and thus function  $T(u)$  can be determined by solving this ordinary differential equation (ODE) using boundary conditions  $T(0) = \sigma_{\min}$ ,  $T(1) = \sigma_{\max}$ .

For any sequence of differentiable parameterized probabilities it can be shown that

$$\psi(\sigma) = \frac{1}{\ln(2)H(\sigma)} \sum_{n=-\infty}^{\infty} \frac{1}{p_n(\sigma)} \left[ \frac{dp_n(\sigma)}{d\sigma} \right]^2, \quad (15)$$

and for normal pdf we have

$$\psi(\sigma) = \frac{1}{\ln(2)H(\sigma)} \left\{ \frac{[\phi_1(\sigma)]^2}{1 - \omega_1(\sigma)} + \sum_{n=1}^{\infty} \frac{[\phi_{2n-1}(\sigma) - \phi_{2n+1}(\sigma)]^2}{\omega_{2n-1}(\sigma) - \omega_{2n+1}(\sigma)} \right\}, \quad (16)$$

where

$$\omega_k(\sigma) \stackrel{\text{def}}{=} \text{erfc}\left(\frac{k}{\sqrt{8}\sigma}\right), \quad \phi_k(\sigma) \stackrel{\text{def}}{=} \frac{k e^{-k^2/(8\sigma^2)}}{\sqrt{2\pi}\sigma^2}. \quad (17)$$

## 4. EXPERIMENTAL RESULTS

The ODE of eq. (14) was solved using the 4th-order Runge-Kutta method [17, §17.1], and boundary conditions  $\sigma \in [0.1, 1000]$ . The solution  $T(u)$  is shown in Fig. 7. A quick observation may lead to the incorrect conclusion that it can be approximated by a function like  $10^{4u^2-1}$  (red line).

Since  $T(u)$  is defined by a differential equation, the quality of the approximation must be measured by relative errors of derivatives. Those are shown in Fig. 8, where we can

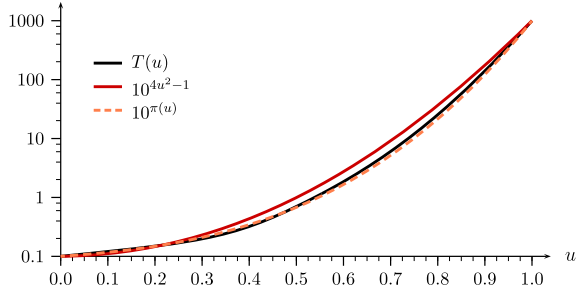


**Fig. 7.** The optimal pdf parameter conversion function  $T(u)$  and two approximations.

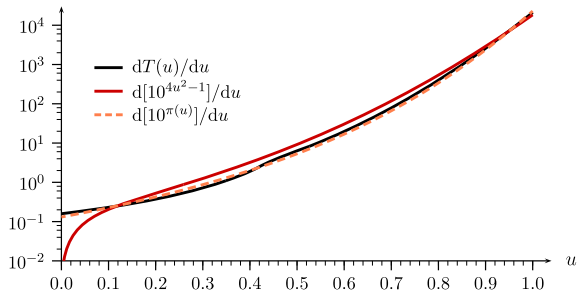


**Fig. 8.** Derivatives of pdf parameter conversion function  $T(u)$  and its approximations.

also see a much better approximation  $T_{\pi}(u) = 10^{\pi(u)}$ , where polynomial

$$\pi(u) = 2.49284 u^3 + 0.93703 u^2 + 0.57013 u - 1, \quad (18)$$

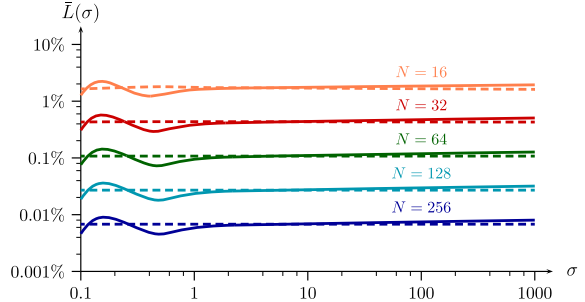
minimizes the maximum relative derivative error.

Fig. 9 shows how the average relative redundancy  $\bar{L}(\sigma)$  varies with  $\sigma$  when uniform quantization is applied to pdf parameter  $u$ , and  $N$  code vectors are used for entropy coding latent variables  $y$ , as shown in Fig. 5. Following the condition defined by eq. (13),  $\bar{L}(\sigma)$  does not change when  $T(u)$  is used for pdf parameter conversion. On the other hand, there are relatively small variations when approximation  $T_{\pi}(u)$  is used instead, and those deviations correspond to errors in approximating the derivatives (cf. Fig. 8).

We also observe that the curves are nearly perfectly parallel, confirming the predominance of the quadratic term in the Taylor series of the relative redundancy. This is also verified by the fact that  $\bar{L}(\sigma)$  quadruples when the  $N$  is halved.

Non-uniform quantizations defined by transformation  $T(u)$  were used for entropy coding values from a floating-point implementation of the scale hyperprior codec [15], in the Kodak image dataset [18]. Redundancy results are shown in Table 1, for average bit rates between 0.25 and 2.5 bits/pixel.

For values of  $N$  larger than about 128 (7 bit representation) the redundancy from quantization is 0.01% or below, which is within the experimental variation. For smaller values of  $N$  we can observe that



**Fig. 9.** Average relative redundancies from  $T(u)$  (dashed) and approximation  $10^{\pi(u)}$  (solid), for different number of quantization intervals  $N$ .

**Table 1.** Coding results obtained using scale hyperprior codec applied to 24 images of Kodak dataset.

$N$	CV mem. (Kbytes)	Rel. redundancy (%) @ bit rate				
		0.25	0.50	1.00	1.50	2.50
256	51.6	0.00	0.00	0.00	0.00	0.01
192	38.7	0.00	0.00	0.00	0.01	0.01
128	25.8	0.04	0.04	0.04	0.03	0.03
96	19.4	0.03	0.04	0.04	0.04	0.05
64	12.9	0.13	0.12	0.12	0.12	0.11
48	9.7	0.24	0.23	0.22	0.22	0.20
32	6.5	0.38	0.38	0.40	0.41	0.42
24	4.9	0.85	0.81	0.81	0.82	0.79
16	3.4	1.79	1.76	1.76	1.78	1.75

- The redundancies are practically constant for all bit rates, meaning that the proposed coding method achieves the design objective of having constant relative redundancies.
- The average redundancy levels  $\bar{L}(\sigma)$  match those of Fig. 9, showing that features predicted by theory match the practical implementation.

The second column of Table 1 contains the total amount of memory needed to store the code vectors, when using 16 bits/element. This shows that the proposed method can be directly used to minimize memory. For example, even if the network is able to support 8 bit outputs, and redundancy below 0.5% is acceptable, the pdf parameter can be further quantized to 5 bits, by simply discarding the 3 least significant bits, to reduce CV memory from 51.6 to 6.5 Kbytes.

## 5. CONCLUSIONS

It is shown that the effects of quantization on the entropy coding can be analyzed by evaluating coding redundancy, and this can be used for changing the pdf parameter to be learned so that average relative redundancy becomes practically constant. In consequence, networks do not need to be re-trained when the pdf parameter quantization is changed, which we show can also be done intentionally to minimize memory for code tables.

## 6. REFERENCES

- [1] S. Ma, X. Zhang, C. Jia, Z. Zhao, S. Wang, and S. Wang, “Image and video compression with neural networks: a review,” *IEEE Trans. Circuits Syst. Video Technol.*, vol. 30, no. 6, pp. 1683–1698, June 2020, arXiv:1904.03567v2.
- [2] D. Ding, Z. Ma, D. Chen, Q. Chen, Z. Liu, and F. Zhu, “Advances in video compression system using deep neural network: a review and case studies,” *Proc. IEEE*, vol. 109, no. 9, pp. 1494–1520, Mar. 2021, arXiv:2101.06341v1.
- [3] Qualcomm AI Research, “World’s first software-based neural video decoder running HD format in real-time on a commercial smartphone,” URL: <https://www.qualcomm.com/news/onq/2021/06/17/worlds-first-software-based-neural-video-decoder-running-hd-format-real-time>, June. 2021.
- [4] Qualcomm AI Research, “Demonstration of real time neural video decoding on a mobile device,” URL: <https://www.youtube.com/watch?v=WUnlSHenr08>, Dec. 2021.
- [5] J. Ascenso, P. Akyazi, F. Pereira, and T. Ebrahimi, “Learning-based image coding: early solutions reviewing and subjective quality evaluation,” in *Proc. SPIE 11353, Optics, Photonics and Digital Tech. for Imaging Applicat. VI*, Apr. 2020, pp. 164–176.
- [6] M. Nagel, M. van Baalen, T. Blankevoort, and M. Welling, “Data-free quantization through weight equalization and bias correction,” in *Proc. IEEE/CVF Int. Conf. Comput. Vision*, Oct. 2019, pp. 1325–1334, arXiv:1906.04721v3.
- [7] M. Nagel, M. Fournarakis, R. A. Amjad, Y. Bondarenko, M. van Baalen, and T. Blankevoort, “A white paper on neural network quantization,” arXiv:2106.08295v1, June 2021.
- [8] T. Liang, J. Glossner, L. Wang, S. Shi, and X. Zhang, “Pruning and quantization for deep neural network acceleration: a survey,” *Neurocomputing*, vol. 461, pp. 370–403, Oct. 2021, arXiv:2101.09671.
- [9] G. J. Sullivan, J.-R. Ohm, W.-J. Han, and T. Wiegand, “Overview of the High Efficiency Video Coding (HEVC) Standard,” *IEEE Trans. Circuits Syst. Video Technol.*, vol. 22, no. 12, pp. 1649–1668, Dec. 2012.
- [10] V. Sze and D. Marpe, “Entropy coding in HEVC,” in *High Efficiency Video Coding (HEVC): Algorithms and Architectures*, V. Sze, M. Budagavi, and G. J. Sullivan, Eds., chapter 8, pp. 209–274. Springer, 2014.
- [11] B. Bross, Y.-K. Wang, Y. Ye, S. Liu, J. Chen, G. J. Sullivan, and J.-R. Ohm, “Overview of the versatile video coding (VVC) standard and its applications,” *IEEE Trans. Circuits Syst. Video Technol.*, vol. 31, no. 10, pp. 3736–3764, Oct. 2021.
- [12] P. Elias, “Universal codeword sets and representations of the integers,” *IEEE Trans. Inf. Theory*, vol. 21, no. 2, pp. 194–203, Mar. 1975.
- [13] A. Said, “Arithmetic coding,” in *Lossless Compression Handbook*, K. Sayood, Ed., chapter 5, pp. 101–152. Academic Press, San Diego, CA, 2003.
- [14] A. Said, “Introduction to arithmetic coding – theory and practice,” Technical Report HPL-2004-76, Hewlett Packard Laboratories, Palo Alto, CA, USA, Apr. 2004, (<http://www.hpl.hp.com/techreports/2004/HPL-2004-76.pdf>).
- [15] J. Ballé, D. Minnen, S. Singh, S. J. Hwang, and N. Johnston, “Variational image compression with a scale hyperprior,” in *Sixth Int. Conf. Learning Representations*, Vancouver, Canada, Apr. 2018, arXiv preprint arXiv:1802.01436v2.
- [16] J. Ballé, N. Johnston, and D. Minnen, “Integer networks for data compression with latent-variable models,” in *Int. Conf. Learning Representations*, New Orleans, Louisiana, USA, May 2019, URL: <https://openreview.net/forum?id=S1zz2i0cY7>.
- [17] W. H. Press, S. A. Teukolsky, W. T. Vetterling, and B. P. Flannery, *Numerical Recipes: The Art of Scientific Computing*, Cambridge University Press, Cambridge, UK, third edition, 2007.
- [18] Kodak Image Dataset, URL: <http://www.cs.albany.edu/~xypan/research/snr/Kodak.html>.